Solvent distributions, solvent orientations and specific hydration regions around 1-adamantyl chloride and adamantane in aqueous solution

Masayuki Ohisa, Misako Aida *

Center for Quantum Life Sciences, and Department of Chemistry,

Graduate School of Science, Hiroshima University, Higashi-Hiroshima, 739-8526

Japan

Abstract

Ab initio molecular orbital theory and Monte Carlo method with molecular mechanics are used to calculate the hydration numbers and solvent configurations around 1-adamantyl chloride in 324 water molecules. In the highest probability region for distribution of water molecules, a water molecule forms two hydrogen bonds with Cl and the adamantane skeleton; in the second highest probability region, a water molecule is located at the rear side. The CH…O interaction in the rear side is enhanced by the Cl substitution. The water orientation in the rear side of 1-adamantyl chloride is different from that around a hydrophobic adamantane molecule.

* Corresponding author. FAX: +81-82-424-0725.

e-mail address: maida@hiroshima-u.ac.jp (Misako Aida).

1. Introduction

Solvation plays an important role in organic reactions. It is now possible to calculate changes in the free energy for reactions in solution with a reasonable computational cost [1-3]. To understand the effect of solvation on the reactivities or properties of solute molecules, it is also important to elucidate the distribution of solvent molecules, i.e., the solvation pattern. In particular, water molecules can form a vast variety of hydrogen bond patterns even with several water molecules at finite temperature [4]. Therefore, a suitable statistical method is required to treat the hydration at finite temperature. There have been several reports with a focus on solvation patterns: three-dimensional distributions of solvents around organic molecules by modified RISM [5], 3D-RISM [6], and molecular dynamics (MD) simulation [7], two-dimensional distributions of water molecules for dissociation of electrolyte by MD simulation [8-11], and those around adamantane dimer as a hydrophobic molecule by MD simulation [12].

A substituted adamantane molecule is often used as a reference species [13, 14] for elucidating the concept of S_N1 reaction [15], in which solvation plays a crucial role. It was shown that the hydrolysis rate constant of 1-adamantyl chloride in aqueous solution increases as the water ratio in solution increases [16]. However, the characteristics of the solvation pattern of substituted adamantane, such as the effect of a substituent on the solvation pattern, need further investigation.

In this letter, we show the hydration numbers and the hydration configurations of 1-adamantyl chloride and adamantane in aqueous solution with the Monte Carlo (MC) simulation which can treat specific interactions between solute and solvent molecules and between solvent molecules and can cover a wide configuration space more easily

than the MD simulation. To visualize the water distribution around the solute, we calculate a number density map of solvents, in which the configuration space is reduced to a two-dimensional space around the solute using a cylindrical coordinate system. This number density map is different from a radial distribution function, in which the configuration space is reduced to a one-dimensional space. To visualize the orientations of water molecules around the solute, we calculate the average dipole-moment arrows of solvent water molecules.

2. Computational methods

Water molecules were distributed around 1-adamantyl chloride in the following manner. First, an ab initio molecular orbital (MO) theory was employed to obtain the geometry of 1-adamantyl chloride, which has C_{3v} symmetry in the isolated state, using the HF/6-31G(d) level of theory. The stationary structure of 1-adamantyl chloride was confirmed by means of a normal mode analysis. The volume occupied by 1-adamantyl chloride was obtained as that inside a contour of 1×10^{-3} electrons bohr^{-3} density. Second, 324 water molecules were distributed around 1-adamantyl chloride in a solvation sphere with a radius of 13.5 Å. The density of water molecules in this sphere excluding the volume occupied by 1-adamantyl chloride is 0.96 g cm^{-3}. Third, we generated 1.296×10^{9} solvent configurations using the MC method with molecular mechanics (MM) to create a canonical ensemble at T = 298 K, in which all molecules were treated as MMs and the energies of electrostatic and the Lennard-Jones interactions between the solute and the solvent molecules were calculated using the following parameters. The charges from the electrostatic potentials were calculated using a grid-based method (CHELPG) [17] at the solute structure using the HF/6-31G(d) level of theory. The

Lennard-Jones parameters determined by Gao [18] were applied to the solute molecule. The TIP3P water potential functions [19] were employed for the solvent molecules.

The Gaussian 03 [20] program package was used for the first part of the above procedure; the program package of HONDO 2004 [21] was used for the second and the third parts of the procedure. One of the configurations of 324 water molecules around 1-adamantyl chloride is displayed in Figure 1.

To observe the distribution of water molecules around the solute, we calculated the number density of the water molecules around the solute. We define the coordinate space using a cylindrical coordinate system. The x axis corresponds to the C_3 axis of 1-adamantyl chloride, and the C atom of C–Cl is placed at the origin (0, 0). The values on the y axis correspond to the radius of the cylinder. The number density $n(x,y)$ of the solvent is expressed as follows:

$$n(x,y) = \frac{\langle N(x,\delta x,y,\delta y)\rangle}{\pi((y+\delta y)^2 - y^2)\delta x} \quad . \qquad (1)$$

The $\langle N(x,\delta x,y,\delta y)\rangle$ denotes the count average of the solvent O atom in x~$x+\delta x$ and y~$y+\delta y$ over 4×10^6 samples, which were selected every 324 MC steps from the generated 1.296×10^9 configurations. The number density is in count $Å^{-3}$.

A similar simulation procedure was performed for adamantane. The geometry of adamantane was optimized with T symmetry in the isolated state, using the HF/6-31G(d) level of theory. To set the same density of water molecules (0.96 g cm^{-3}, excluding the volume occupied by adamantane) in the same radius of the solvaton sphere (13.5 Å) for adamantane as for 1-adamantyl chloride, 325 water molecules were distributed around adamantane. Then, we generated 1.3×10^9 solvent configurations to create a canonical ensemble at T = 298 K. The number density map of water molecules around adamantane was drawn as described above. To obtain the count average of

solvent O atoms, we used 4×10^6 samples, which were selected every 325 MC steps from the generated 1.3×10^9 configurations

To observe the orientations of water molecules around the solute, we used average dipole-moment arrows. A vector is so defined that it indicates the bisector of the H-O-H angle of a water molecule and corresponds to the dipole moment of the water molecule. To treat the water orientations statistically, first, all vectors which appeared in a cubic cell of $(0.5\ \text{Å})^3$ in the 4×10^6 MC samples were summed up. Secondly, the total vectors in the neighboring 3×3×3 cells were averaged. The obtained averaged vector was then used as the average dipole-moment arrow of the cubic cell.

The binding energies between 1-adamantyl chloride and a water molecule, between adamantane and a water molecule, and between water molecules were calculated using the Gaussian 03 program package [20] at the theoretical level of MP2/aug-cc-pVDZ with the basis set superposition error (BSSE) being corrected. The BSSE was evaluated using the counterpoise method. Electrostatic maps of 1-adamantyl chloride and adamantane were calculated with MP2/aug-cc-pVDZ. All the geometries in this part were optimized with MP2/aug-cc-pVDZ.

3. Results and discussion

3.1. *Number density map of water*

The map of the number density $n(x,y)$ of water molecules around 1-adamantyl chloride is shown in Figure 2(a), where the first solvation shell of 1-adamantyl chloride can be observed. We count the number of water molecules in the first solvation shell of the solute. Here, we define the first solvation shell as a region that contains the first peak of the probability of solvent O atoms. The number of solvent molecules in the first

solvation shell of the adamantane skeleton was obtained by counting the number of water molecules within 6.0 Å from the center of the adamantane skeleton. The first solvation shell of the Cl atom is defined as the region within 5.0 Å from the Cl atom and the region where arctan(b/a) > arctan(3.2/[−3.7−(−1.8)]). Here, note that the Cl atom is at (−1.822, 0). The region in the first solvent shell common to the Cl atom and the adamantane skeleton, which corresponds to the region around (−2.0, 3.9), is defined as the region within 5.0 Å from the Cl atom, where arctan(b/a) ≤ arctan(3.2/[−3.7− (−1.8)]) and x < −0.9 Å. Here, 0.9 Å corresponds to half of the C−Cl bond length, 1.822 Å. The rear side of 1-adamantyl chloride, which is reverse to the Cl atom, is defined as 5.3 ≤ x < 7.2 Å and y < 2.0 Å. The total numbers of water molecules in the regions of the Cl atom, the adamantane skeleton, the common region, and the rear side were calculated to be 4.4, 25.7, 6.5, and 1.2, respectively, for the first solvation shell of 1-adamantyl chloride. The total number of water molecules around the entire solute is calculated by adding the number of water molecules that are present in the first solvation shell of the adamantane skeleton or the Cl atom. This number was calculated to be 30.1. The density in the first solvent shell was 1.28 g cm^{-3}, which is larger than the net density of water molecules, i.e., 0.96 g cm^{-3}, in this study.

Experimentally, the number of excluded water molecules from the association between β-cyclodextrin and 1-adamantanecarboxylic acid [22] and that between β-cyclodextrin and adamantanecarboxylate [23] were 20 ~ 25 and 15 ~ 25, respectively. The number of water molecules around the adamantane skeleton, 25.7, in the present study is comparable to these numbers.

The map of the number density $n(x,y)$ of water molecules around adamantane is shown in Figure 2 (b). The number of solvent molecules in the first solvation shell of

adamantane was calculated to be 28.6, which was obtained by counting the number of water molecules within 6.0 Å from the center of the adamantane skeleton. The density in the first solvent shell was 1.21 g cm^{-3} which is lower than the first solvent shell of 1-adamantyl chloride (1.28 g cm^{-3}) and larger than the net density (0.96 g cm^{-3}) of water molecules in the current simulation. The increase in the water density around adamantane compared to that of bulk water may indicate that specific interactions occur between the hydrophobic solute and the surrounding water molecules and that the solute affects the distribution of the water molecules. The increase in the local solvent density may generate negative hydration energy and negative hydration entropy, both of which together are the characteristics of hydrophobic hydration [24].

In comparison of the number density map of 1-adamantyl chloride (Figure 2 (a)) with that of adamantane, Figure 2 (b), the Cl substitution changes the water distribution around the adamantane skeleton in the region near the Cl atom, as well as in the region of the rear side. Especially, the change in the rear side is remarkable, since this region is obviously far from the substitution point. In Figure 2(c), the number density $n(x, 0)$ of water O atoms in the rear side of 1-adamantyl chloride ($5.0 \leq x < 9.0$ Å) is plotted together with that in the corresponding region of adamantane. It is worthy of note that the peak of O distribution is higher and closer to the adamantane skeleton in the rear side in 1-adamantyl chloride than in adamantane. Furthermore, there is a remarkable difference in the directions of the water molecules in this region of 1-adamantyl chloride. In the rear side of 1-adamantyl chloride, Figure 3(a), we find that the average dipole-moment arrows are directed toward the normal, while those are tangential to the surface of the adamantane skeleton in the corresponding region of adamantane, Figure 3(b). A snapshot of a representative water direction in the rear side of 1-adamantyl

chloride, shown in Figure 4(a), corresponds to the arrow directions in Figure 3(a), and another snapshot of a representative water direction in the corresponding region of adamantane is displayed in Figure 4(b).

3.2. *Water orientations around solute*

The average dipole-moment arrows in the first solvent shell of 1-adamantyl chloride are plotted in Cartesian coordinates in Figure 5(a), and those of adamantane in Figure 5(b). Around adamantane, the water molecules in the first solvent shell are oriented in such a way that the dipole directions of water are tangential to the skeleton surface, and the hydrogen bonding network is formed among the water molecules in the first shell as well as between the first shell and the outer shell. The surface of 1-adamantyl chloride is covered with tangential water molecules, except in the region near the Cl atom and in the rear side. In the region near the Cl atom, the H atoms of water molecules are directed toward the Cl atom.

Analyses of neutron diffraction data have shown that water molecules form a disordered hydrogen-bonded cage around methanol [25], methane [26] and the hydrophobic group of *tert*-butanol [27] and that the water molecules being located in the hydrophobic region and involved in the hydration take the tangential orientation to the hydrophobic surface, whereas those molecules located close to the hydrophilic hydroxyl group adopt hydrogen-bonding configurations. In our present simulations, we have observed similar orientations of the water molecules around adamantane as well as those around 1-adamantyl chloride. The differences in the local water orientations between adamantane and 1-adamantyl chloride are found in the region near the Cl atom and in the rear side of 1-adamantyl chloride; see Figures 5(a,b).

Note that the average dipole-moment arrows may vanish, except for those in the regions along the C_3 axis of 1-adamantyl chloride, if the MC simulation is performed in very large steps. Nevertheless, the distribution of the average dipole-moment arrows in the current MC simulation is meaningful and indicative of characteristic orientations of water networks around the solute. Along the C_3 axis in the rear side of 1-adamantyl chloride, it is probable that the average dipole-moment arrows do not vanish and the characteristic orientation of water is always observed, because the reversal of the orientation of a water molecule, such that the vector is directed toward a solulte molecule in this region, should be very exceptional. Along the C_3 axis in the Cl hydration region of 1-adamantyl chloride, the same is true as in the rear side, because reversal of the orientation of a water molecule in this region turning the vector against the solute, should also be very exceptional.

3.3. *Solute-water C–H…O interaction*

The electrostatic maps of 1-adamantyl chloride and adamantane at the MP2/aug-cc-pVDZ level of theory are shown in Figure 6. The map for 1-adamantyl chloride, where $\delta-$ around the Cl atom and $\delta+$ around the adamantane skeleton are shown, indicates that specific interactions can occur not only between the Cl atom and a water H atom but also between an H atom of the adamantane skeleton in the rear side and a water O atom. The dipole moment of 1-adamantyl chloride is calculated to be 3.01 debyes (MP2/aug-cc-pVDZ). It is noteworthy that the average directions of the water molecules located in the rear side of 1-adamantyl chloride, Figure 3(a), correspond to the favorable dipole-dipole interaction between the solute and solvent.

For quantitative investigation of the interactions between 1-adamantyl chloride and a water molecule, the binding energy between these molecules and that between the water molecules were calculated using the MP2/aug-cc-pVDZ level of theory, with BSSE being corrected. We found two characteristic stable regions for the interactions between 1-adamantyl chloride and a water molecule under the constraint of the C_s symmetry, as shown in Figure 7(a). The first stable region is located around the Cl atom. The distances of H...Cl and O...H–C are 2.417 and 2.532 Å, respectively. The binding energy E_{bind} between 1-adamantyl chloride and a water molecule in the first stable region is 3.95 kcal mol^{-1}, which is comparable to that of water dimer (4.42 kcal mol^{-1}). The second stable region is located at the rear side of 1-adamantyl chloride. The distances of O...H–C are 2.612 and 2.757 Å, which are longer than those obtained in the first case. The binding energy of a water molecule to 1-adamantyl chloride in the second stable region is 1.39 kcal mol^{-1}. The binding energy of a water molecule to adamantane at the position corresponding to the second stable region for 1-adamantyl chloride is 0.92 kcal mol^{-1}, as shown in Figure 7(b). It is remarkable to note that the Cl atom enhances the binding energy between the adamantane skeleton and a water molecule even in the rear side. This enhancement may correspond to the difference in the water O atom distributions, as shown in Figure 2(c), and also to the difference in the water orientations, as shown in Figure 3. Similar results were obtained for benzene and hexafluorobenzene in aqueous solution [28], where the fluorine atom affects the water distribution and orientation not only around the fluorine itself but also in the axial regions.

In tetrahydrofuran-water mixtures, the C–H...O interaction was observed using NMR and IR [29], and it was proposed that the formation of weak C–H…OH_2

hydrogen bonds was responsible for the hydrophobic hydration of tetrahydrofuran. The present calculations indicate that the C–H…O interaction is enhanced by halogen substitution even in the rear side of a large hydrophobic skeleton. This enhancement had been recognized in smaller molecules: C–H...O binding energies between a water molecule and H_3CH, FH_2CH, and F_2HCH are 0.43, 1.23, and 2.24 kcal mol^{-1}, respectively, at the MP2/aug-cc-pVDZ level of theory [30]. The interaction between C–H of a hydrophobic skeleton and a water O atom is considered as a C–H...O interaction, and this is enhanced by halogen substitution. The interactions between the hydrophobic skeleton and water molecules found in the present calculations may be of significance for understanding of hydration phenomena of hydrophobic molecules.

4. Conclusion

Two-dimensional number density maps of water oxygen atoms and average dipole-moment arrows of water molecules are useful in clarifying the hydration pattern around a bulky solute such as 1-adamantyl chloride and adamantane. The total number of water molecules around the entire 1-adamantyl chloride and that around adamantane in the first solvent shell are 30.1 and 28.6, respectively. The water density of the first solvent shell around 1-adamantyl chloride is slightly higher than that around adamantane and is much higher than that of the net water density. The region of the highest probability region of water molecules around 1-adamantyl chloride is located around the region common to the Cl atom and the adamantane skeleton, while the second highest one is located at the rear side of 1-adamantyl chloride. The C–H…O interaction between C–H of adamantane skeleton and water O atom is enhanced by the Cl substitution of the adamantane skeleton even in the rear side. In the rear side of

1-adamantyl chloride, the average dipole-moment arrows of water molecules are directed toward the normal of the surface. By comparing the number density maps of the water oxygen and the water orientation pattern in the first solvent shell of 1-adamantyl chloride to those of adamantane, we conclude that both of the negative excess hydration energy and the negative excess hydration entropy at 298 K are larger in aqueous solution of 1-adamantyl chloride than in that of adamantane.

Acknowledgement

This work was supported in part by a Grant-in-Aid for Scientific Research from the Ministry of Education, Culture, Sports, Science and Technology of Japan. The calculations were carried out at the Center for Quantum Life Sciences (QuL*i*S) and at the Research Center for Computational Science, Okazaki National Research Institutes.

References

[1] M. Ohisa, H. Yamataka, M. Dupuis, M. Aida, Phys. Chem. Chem. Phys. 10 (2008) 844.

[2] W.L. Jorgensen, J.K. Buckner, S.E. Huston, P.J. Rossky, J. Am. Chem. Soc. 109 (1987) 1891.

[3] Encyclopedia of Computational Chemistry, Wiley, Chichester, West Sussex, 1998, p. 1070.

[4] T. Miyake, M. Aida, Chem. Phys. Lett. 363 (2002) 106.

[5] D. Yokogawa, H. Sato, T. Imai, S. Sakaki, J. Chem. Phys. 130 (2009) 064111.

[6] C. Chiappe, M. Malvaldi, C.S. Pomelli, J. Chem. Theory Comput. 6 (2010) 179.

[7] T. Takamuku, M. Tanaka, T. Sako, T. Shimomura, K. Fujii, R. Kanzaki, M. Takeuchi,

J. Phys. Chem. B 114 (2010) 4252.

[8] X. Li, L. Gong, Z. Yang, Sci. China, Ser. B Chem. 51 (2008) 1221.

[9] Z. Zhang, Z. Duan, Chem. Phys. 297 (2004) 221.

[10] C.J. Fennell, A. Bizjak, V. Vlachy, K.A. Dill, J. Phys. Chem. B 113 (2009) 6782.

[11] K. Yui, M. Sakuma, T. Funazukuri, Fluid Phase Equilib. 297 (2010) 227.

[12] M. Makowski, C. Czaplewski, A. Liwo, H.A. Scheraga, J. Phys. Chem. B 114 (2010) 993.

[13] F.L. Schadt, T.W. Bentley, P.v.R. Schleyer, J. Am. Chem. Soc. 98 (1976) 7667.

[14] T.W. Bentley, C.T. Bowen, D.H. Morten, P.v.R. Schleyer, J. Am. Chem. Soc. 103 (1981) 5466.

[15] C.K. Ingold, Structure and Mechanism in Organic Chemistry, 2nd ed., Cornell University Press, Ithaca, NY, 1969.

[16] T.W. Bentley, G.E. Carter, J. Am. Chem. Soc. 104 (1982) 5741.

[17] C.M. Breneman, K.B. Wiberg, J. Comput. Chem. 11 (1990) 361.

[18] M. Freindorf, J. Gao, J. Comput. Chem. 17 (1996) 386.

[19] W.L. Jorgensen, J. Chandrasekhar, J.D. Madura, R.W. Impey, M.L. Klein, J. Chem. Phys. 79 (1983) 926.

[20] M.J. Frisch, et al. Gaussian 03, Revision C.02, Gaussian, Inc., Pittsburgh, PA, 2003.

[21] M. Dupuis, HONDO 2004, based on HONDO95, available from the Quantum Chemistry Program Exchange.

[22] N. Taulier, T.V. Chalikian, J. Phys. Chem. B 110 (2006) 12222.

[23] D. Harries, D.C. Rau, V. A. Parsegian, J. Am. Chem. Soc. 127 (2005) 2184.

[24] B. Guillot, Y. Guissani, S. Bratos, J. Chem. Phys. 95 (1991) 3643.

[25] A.K. Soper, J.L. Finney, Phys. Rev. Lett. 71 (1993) 4346.

[26] C.A. Koh, R.P. Wisbey, X. Wu, R.E. Westacott, J. Chem. Phys. 113 (2000) 6390.

[27] D.T. Bowron, A.K. Soper, J.L. Finney, J. Chem. Phys. 114 (2001) 6203.

[28] M. Allesch, E. Schwegler, G. Galli, J. Phys. Chem. B 111 (2007) 1081.

[29] K. Mizuno, Y. Masuda, T. Yamamura, J. Kitamura, H. Ogata, I. Bako, Y. Tamai, T. Yagasaki, J. Phys. Chem. B 113 (2009) 906.

[30] S. Scheiner, Theory and Applications of Computational Chemistry: The First Forty Years, Chapter 29, Elsevier, Amsterdam, 2005.

Figure captions

Figure 1. Configuration of 324 water molecules around 1-adamantyl chloride in a sphere with a radius of 13.5 Å.

Figure 2. (a) Map of the number density $n(x,y)$ of water oxygen atoms around 1-adamantyl chloride ($-6.4 \le x < 10.0$ Å, $\delta x = 0.1$ Å, $0.0 \le y < 6.0$ Å and $\delta y = 0.1$ Å in Eq. (1)); (b) Map of number density $n(x,y)$ around adamantane ($-5.7 \le x < 10.0$ Å, $\delta x = 0.1$ Å, $0.0 \le y < 6.0$ Å and $\delta y = 0.1$ Å in Eq. (1)); (c) The number density $n(x, 0)$ of water oxygen atoms in the rear side for 1-adamantyl chloride (○ in pink) and adamantane (□ in blue) ($5.0 \le x < 9.0$ Å, $\delta x = 0.1$ Å, $y = 0$ Å and $\delta y = 1.0$ Å in Eq. (1)).

Figure 3. (a) Average dipole-moment arrows of water molecules in the rear side of 1-adamantyl chloride plotted in Cartesian coordinates for $5.25 \le x < 7.25$ Å, $-0.25 \le y < 0.25$ Å and $-1.25 \le z < 1.25$ Å. (b) The same plot for adamantane.

Figure 4.. Snapshots of (a) the nearest 30 water molecules around 1-adamantyl chloride in a view from the rear side, and (b) the nearest 28 water molecules around adamantane.

Figure 5. (a) Average dipole-moment arrows of water molecules in the first solvent shell of 1-adamantyl chloride plotted in Cartesian coordinates. To make a complicated and overlapped view clear, only the arrows larger than 25367 debyes, are drawn. (b) The same plot for adamantane.

Figure 6. Electrostatic potential maps with the MP2/aug-cc-pVDZ level of theory: (a) 1-adamantyl chloride and (b) adamantane. The values are in a.u.

Figure 7. Optimized structures under the constraint of C_s symmetry and binding energies E_{bind}: (a) 1-adamantyl chloride and a water molecule, and (b) adamantane and a water molecule. Selected distances (in Å) are indicated.

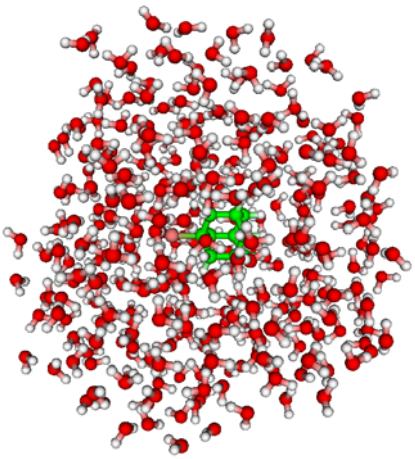

Fig. 1 (Ohisa & Aida)

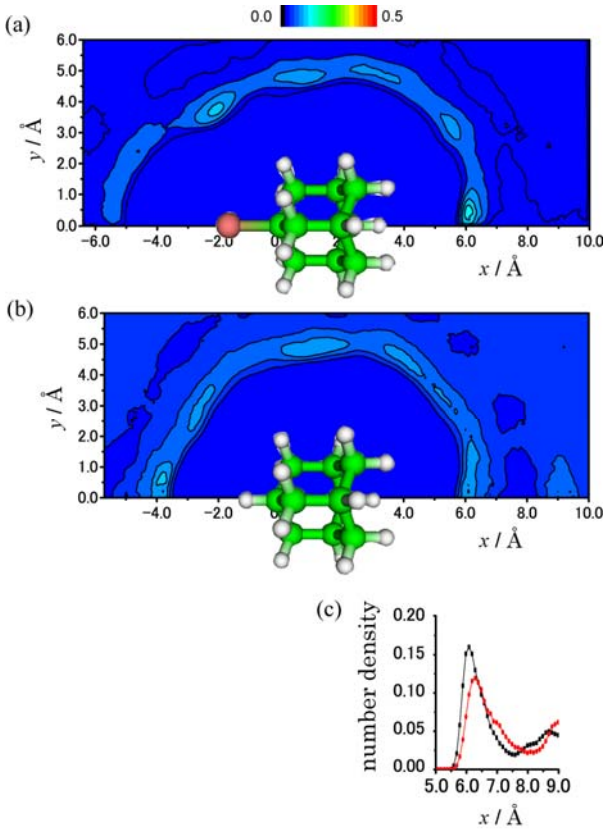

Fig. 2 (Ohisa & Aida)

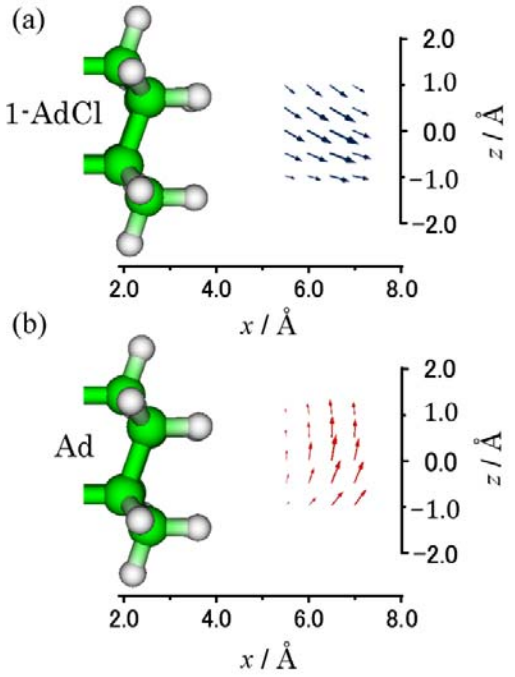

Fig. 3 (Ohisa & Aida)

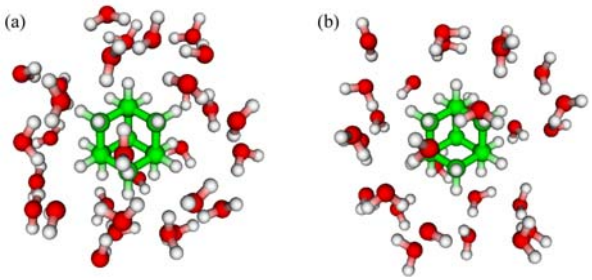

Fig. 4 (Ohisa & Aida)

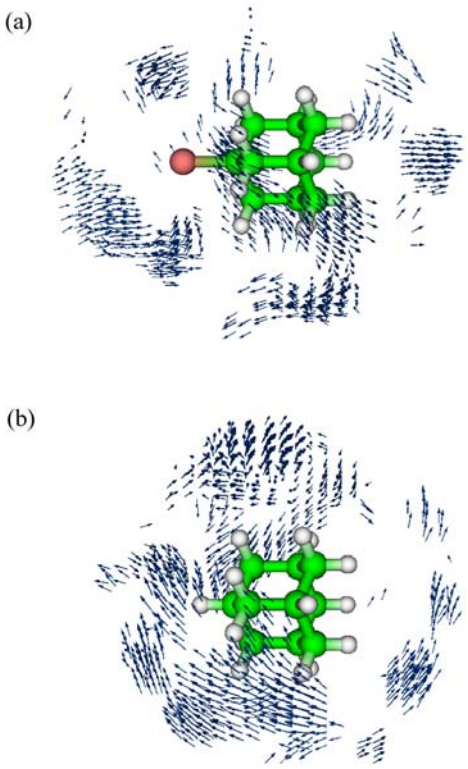

Fig. 5 (Ohisa & Aida)

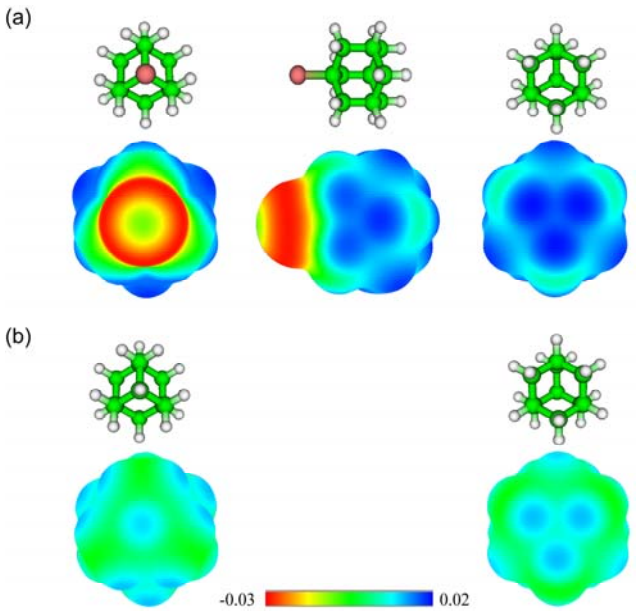

Fig. 6 (Ohisa & Aida)

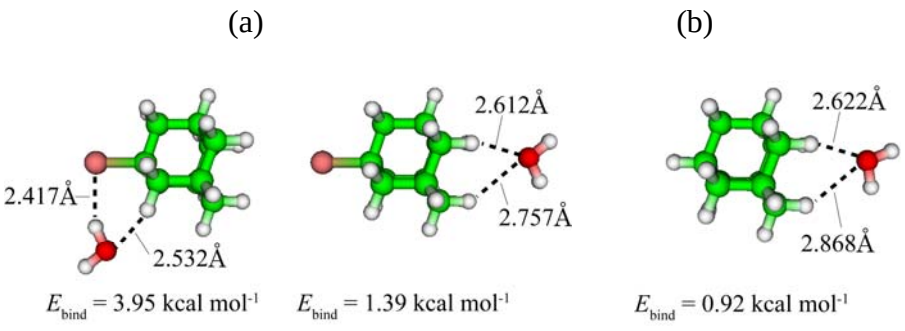

Fig. 7 (Ohisa & Aida)